

The Stability of a Laminated Voussoir Beam: Back Analysis of a Historic Roof Collapse Using DDA

YOSSEF H. HATZOR
RON BENARY

The stability of a horizontally bedded and vertically jointed roof, referred to here as a laminated Voussoir beam, is studied using careful documentation of a historic roof collapse, which occurred in an ancient underground water storage reservoir dated back to ca. 1000 B.C. The roof of the opening failed immediately after the excavation leaving a dome shaped loosened zone, with a span of 7 m and height of 2.5 m, consisting of horizontal beds and vertical joints with mean spacing of 50 and 25 cm, respectively. The ancient engineers erected a massive pillar at the center of the dome in order to passively support the failed roof and the opening remained in service for several hundred years following the failure. Analysis of the roof using iterative Voussoir beam procedure [Beer, G. and Meek, J. L., Design curves for roofs and hanging walls in bedded rock based on Voussoir beam and plate solutions. Trans. Inst. Min. Metall., 1982, 91, A18–22.] shows that the roof was more sensitive to failure by shear along the abutments rather than by crushing at hinge zones and that the required friction angle ($\phi_{req.}$) for stability would have been 36° . The available friction angle is estimated between 38.6° and 46.4° and, therefore, the result of the iterative solution is considered unconservatively wrong. Results of DDA [Shi, G. -H. and Goodman, R. E., Two-dimensional discontinuous deformation analysis. Int. J. Numer. Anal. Methods Geomech., 1989, 13, 359–380; Shi, G. -H., Block System Modeling by Discontinuous Deformation Analysis. Computational Mechanics Publications, Southampton, 1993, pp. 209.] however indicate that $\phi_{req.}$ must have been greater than 60° , a shear strength which was not available at the time of construction, thus the immediate failure. Using DDA we further demonstrate that $\phi_{req.}$ is related to joint spacing (or block length) in a parabolic function: with increasing joint spacing $\phi_{req.}$ decreases to a minimum value and then increases with further increase in joint spacing. This result is attributed to the interaction of two competing forces: one is the stabilizing axial thrust which increases with increasing moment arm in individual blocks (a function of joint spacing or block length), the other is the destabilizing vertical load which increases with increasing weight of overlying blocks. © 1998 Elsevier Science Ltd.

INTRODUCTION

The analysis of a horizontally bedded roof with vertical joints is made complicated by the fact that there is no close form solution for a matrix of individual rock blocks which interact with one another as individual elements. Beam theory can be utilized in the analysis of a horizontally bedded rock and analytical solutions

are available for the shear and axial stress distribution as well as the amount of deflection across the beam, as a function of elastic parameters, density of the rock and geometry of the beam. The design of support pressure for a laminated roof with beds of varying thickness is discussed by Obert and Duvall [1] and incorporation of friction between layers is discussed by Goodman [2], using principles of beam theory. These analyses however are limited to the case of a clamped beam which is not free to displace along the abutments. When the beam consists of a single bed with

Rock Mechanics Laboratory of the Negev, Department of Geology and Mineralogy, Ben-Gurion University of the Negev, P.O. Box 653, Beer-Sheva 84105, Israel.

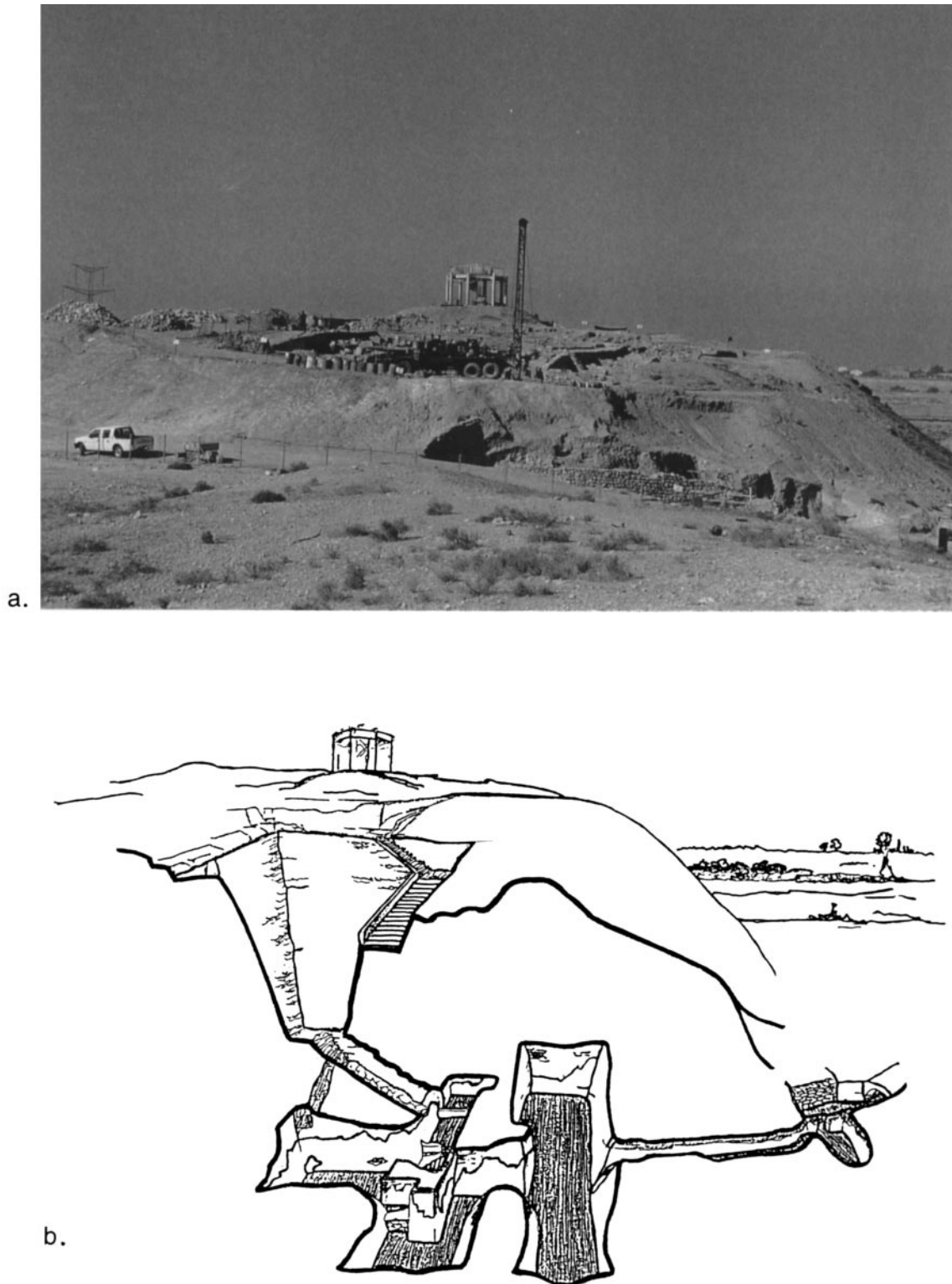


Fig. 1. The water storage system at Tel Beer-Sheva: (a) a photograph of the archeological excavation site and (b) artist conception of the underground opening beneath the archeological site.

vertical joints, the so-called *Voussoir* beam is obtained, and the problem becomes statically indeterminate. In this configuration the jointed beam is free to displace on either the abutments or across midjoints. Evans [3] developed a design procedure for Voussoir beam geometry, a method which was later extended by Beer and Meek [4] and is reviewed in detail by Brady and Brown [5]. The Voussoir beam analysis method is

based on iterations in which initial load distribution and line of action in the system are assumed. The analysis provides the compressive zone thickness and the maximum axial (horizontal) stress, thus, the factor of safety against failure in buckling, axial compression, or shear along the vertical abutments can be calculated, provided that the unconfined compressive strength of the rock and the shear strength of the dis-

continuities are known. The advantage of the Voussoir beam approach is that it allows investigation of a failure mode which has been largely overlooked in the past, namely failure by shear sliding along the abutments. The disadvantages of the method are that only a single layer is modeled and that the influence of spacing and friction between the vertical joints is ignored.

The mechanical strength of a Voussoir beam was tested experimentally and numerically by Passaris *et al.* [6] who have studied the crushing strength of the beam and the mechanism of shear sliding along side walls has been investigated by Ran *et al.* [7]. In both studies the analysis was extended to the case of multiple midjoints and the spacing between joints was considered, but friction along the discontinuities was not modeled.

The real situation however is more complex than the assumed Voussoir beam configuration. Typically the roof of a mine is excavated through sedimentary rock which consists of both horizontal strata and vertical joints, in the most simple case. This basic configuration is referred to here as a *laminated Voussoir beam*. In the general case the strata are inclined and the joints dip at random attitudes. Analytical solutions for the simple, realistic case are not available and numerical methods must be applied. In order to truly simulate deformation characteristics of a laminated Voussoir beam the numerical method should allow rigid body movement and deformation to occur simultaneously, and convergence in every time step should be achieved after relatively large block displacement and rotation, without block penetration or tension. Furthermore, the vertical load which is typically assigned explicitly, must be evaluated and updated implicitly in every time step, since it varies with vertical location in the beam, as well as with the progress of beam deformation. Finally, the model must incorporate the influence of joint friction on block displacement and on the arching mechanism.

In this paper the failure of a laminated Voussoir beam, which occurred at about 1000 B.C. in an underground water storage reservoir at the archeological site of Tel Beer-Sheva, Israel, is back analyzed. All geometrical variables including beam span, beam thickness, joint spacing and bed thickness were determined from careful field mapping and site investigations. The intact rock material properties were determined using servo-controlled constant strain-rate triaxial tests, performed on NX cores retrieved from two bore holes which were drilled especially for the purpose of this study. The beam geometry and intact rock properties are used as input parameters in both classic Voussoir beam analysis [4] and discontinuous deformation analysis [8, 9] and the stability of a laminated Voussoir beam with variable joint spacing and friction is studied.

THE FAILURE OF A LAMINATED ROOF WITH VERTICAL JOINTS - A CASE STUDY

In the archeological site of Tel Beer Sheva (an ancient city dated back to the Iron age 1200–700 B.C., Fig. 1(a)) an underground water storage reservoir dated back to approximately 1000 B.C. was explored (Fig. 1(b)). The excavation of the water system revealed that the roof of the underground opening had collapsed, probably during the time of construction and that the ancient engineers had erected a massive support pillar in the center of the opening in order to support the remaining roof. The same plaster coating which was explored on the opening side walls at ground level was also discovered, higher above the level of the original roof, indicating the proximity of the failure episode to the original time of excavation.

The reservoir was excavated in horizontally bedded chalk with vertical joints clustered in three joint sets (Figs 2 and 3). The most abundant joint sets (J1 and J2, Fig. 3) are orthogonal with mean spacing of 20–25 cm, and the mean bed thickness is about 50 cm, the intersection of which creates a dense network of cubic blocks which form the roof of the excavation (Fig. 4).

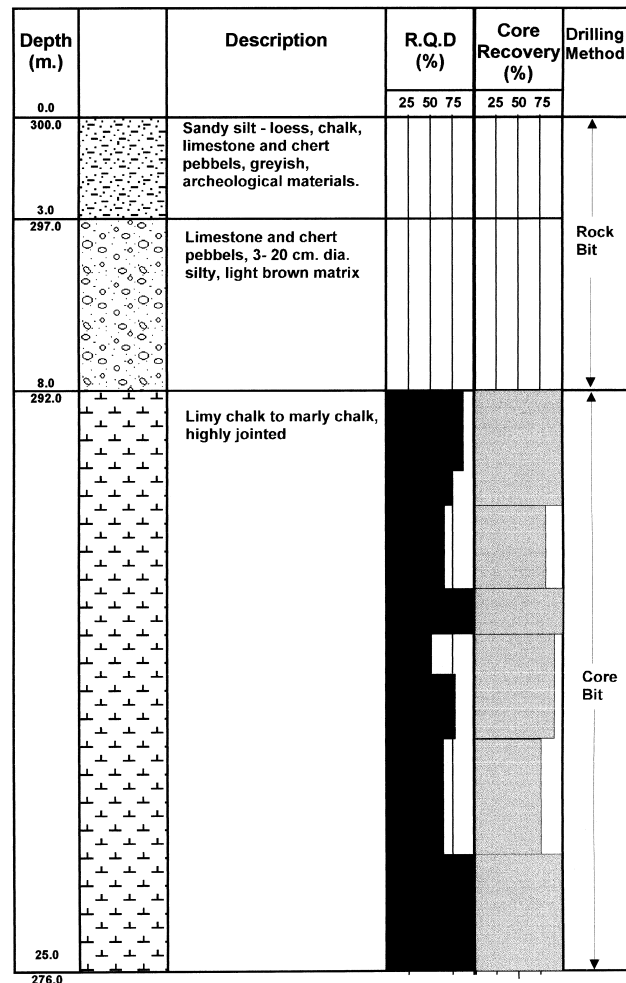


Fig. 2. Drill log showing the stratigraphy and lithological description of the rock units, the % core recovery and the retrieved RQD values.

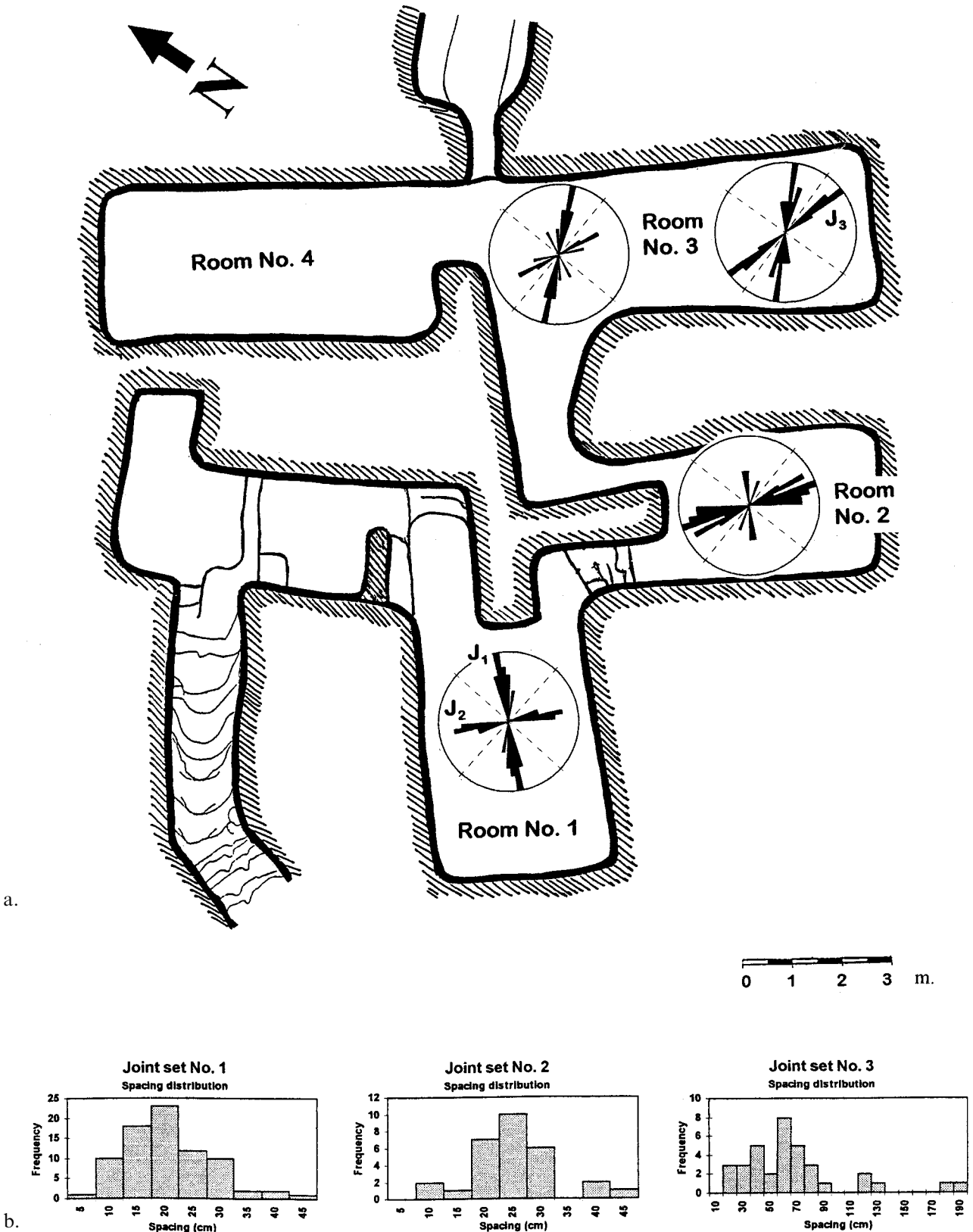


Fig. 3. (a) A map of the underground water storage system with the strike of the joints as mapped underground and (b) joint spacing distribution.

The roof collapsed into the shape of a three-dimensional dome. Five zones were mapped in the roof: zone 1, the original roof level; zone 2, a vertical step with thickness between 50 and 125 cm; zone 3, a sub-horizontal plane parallel to an existing bedding plane;

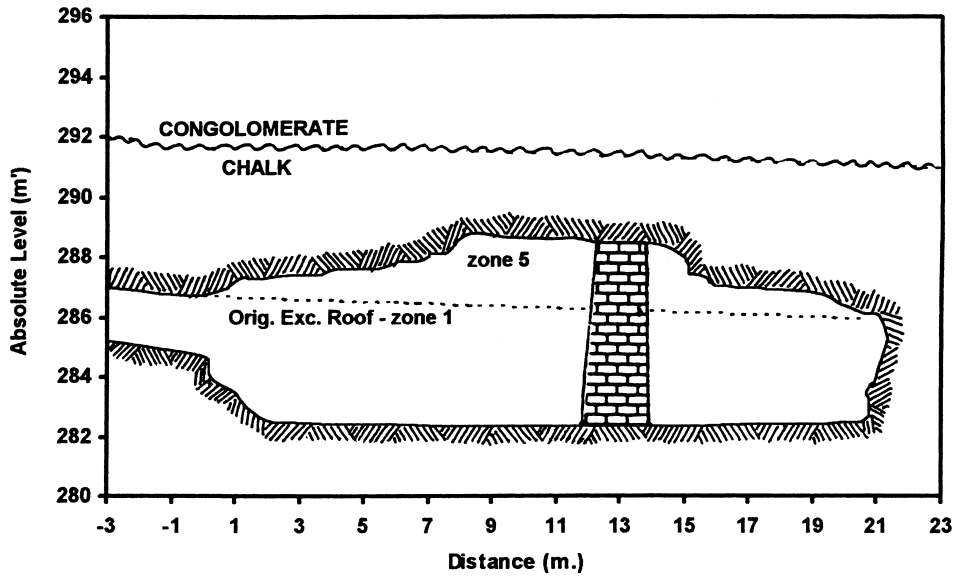
zone 4, a vertical step similar to zone 2 and zone 5, the uppermost failure level which, like zone 3, is parallel to an existing bedding plane (Fig. 5). A structural map of the roof is shown in Fig. 6. It can be seen that the center of the roof is comprised of zone 5 with a



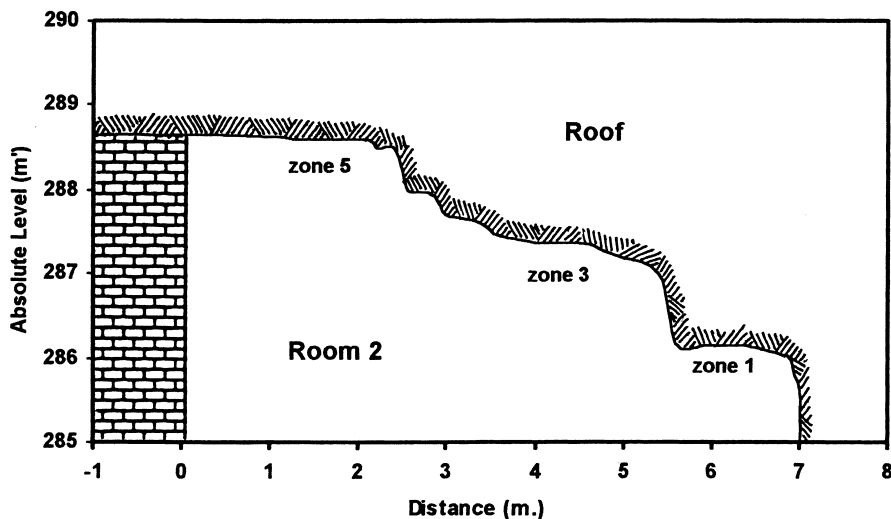
Fig. 4. Photograph collage showing the roof of room 1. The prismatic blocks are formed by members of joint sets 1 and 2 with mean joint spacing of 20 and 25 cm, respectively. The horizontal bed thickness is about 50 cm.

circular boundary, and that the external sections of the roof are comprised of zone 1, the original roof level. The support pillar was erected directly below zone 5 (Fig. 5(a)) and extensions were built in order to support the unstable transitions from zone 5 to 3 (Fig. 6).

The mapped roof is considered here a failed laminated Voussoir beam. In Fig. 7 a typical cross section of only one level in the failed beam is shown. The complete beam consists of several lamina, depending on the bed thickness. The number of lamina is greater



a



b

Fig. 5. Cross sections through the water storage system: (a) longitudinal section showing the ancient support pillar and (b) cross section through room 2 showing the stepped roof after failure. Zone 1 is the original roof with plaster coating, zone 5 is the uppermost surface in the loosened zone, zone 3 is an intermediate level.

then the number of vertical steps since within every major step (zones 2 and 4) several horizontal bedding planes exist.

The failed beam has arrived at a new equilibrium after the collapse, with the aid of support measures taken by the ancient engineers, primarily in the form of the central support pillar (Figs 5 and 6). A partial view of the new roof configuration after the collapse is shown in Fig. 8. The actual problem is therefore completely three-dimensional, although axis-symmetric. In this paper, however, the discussion is limited to two-dimensional analysis only.

Mechanical properties of the rock mass

The ancient excavation was performed in horizontally bedded and vertically jointed chalk of late Cretaceous age. The chalk is covered by 5 m of a well cemented conglomerate and by about 3 m of soil in which the archeological remains are found (Fig. 2 and Fig. 5(a)). The bed thickness in the chalk is between 30 and 80 cm with an average thickness of 50 cm. In between the beds thin marly infilling material is found in places. The RQD values determined from core recovery range between 44 and 100%, with typical

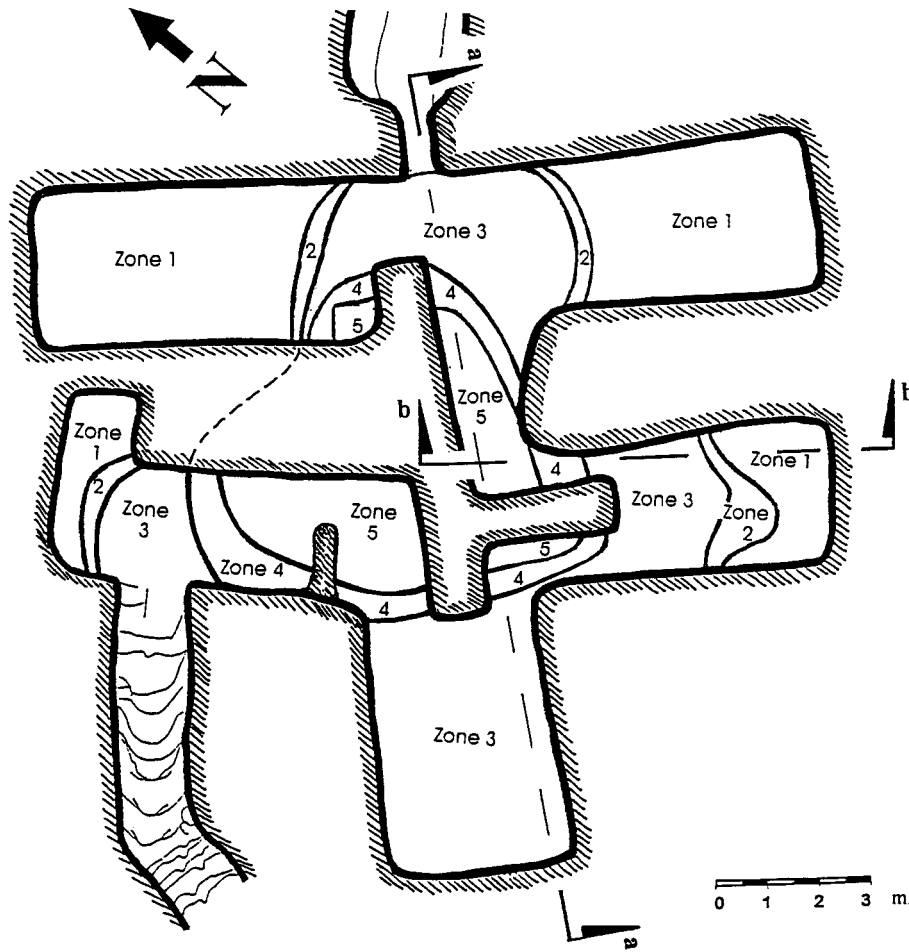


Fig. 6. A structural map of the roof showing the three-dimensional dome which was formed after the failure. The support pillar was erected below the uppermost level of the loosened zone (zone 5), with side extensions designed to support the transition zone (zone 4) between horizontal roof segments.

values between 65 and 80%. The mechanical strength of the chalk and elastic parameters were determined from five triaxial tests which were performed under a constant strain rate of 10^{-5} s^{-1} in a stiff, hydraulic, servo-controlled system. The confining pressures which were used were 0, 2, 4, 6 and 10 MPa. The unconfined compressive strength of the chalk is 7 MPa, the elastic

module (E) and Poisson ratio (ν) as measured in unconfined compression are 2 GPa and 0.1, respectively. A linear Coulomb–Mohr failure envelope fitted to the peak strength values yielded a cohesion of 3.1 MPa and internal friction angle of 32° . The porosity of the chalk is between 27 and 30% and the unit weight is between 18.1 and 20.1 kN/m^3 . The Atterberg

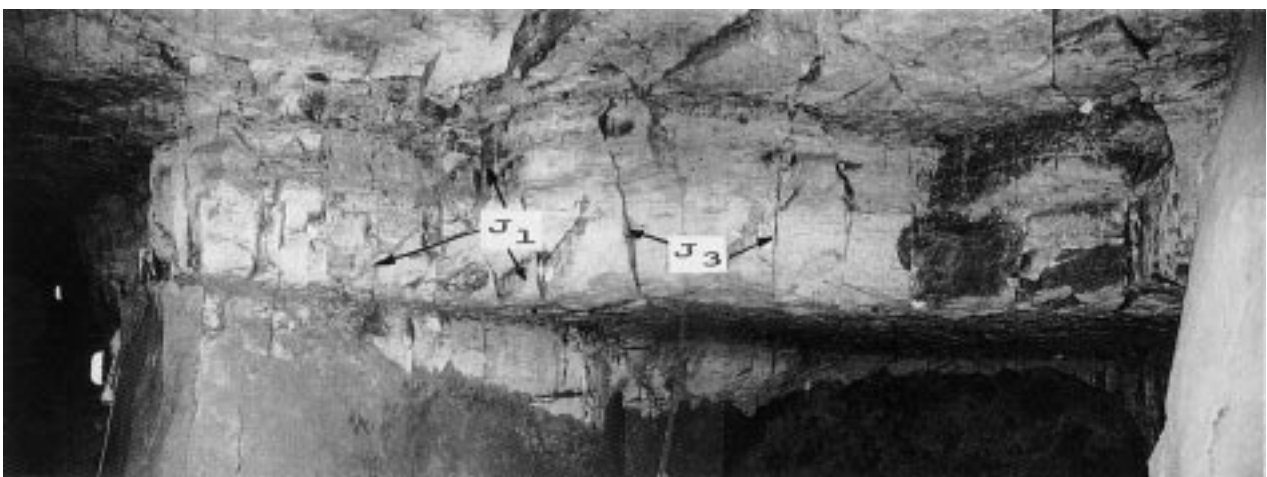


Fig. 7. A photograph showing the roof above room 3 with vertical joints belonging to sets 1 and 3. The plaster coating on the original roof (zone 1) and side walls can still be recognized.

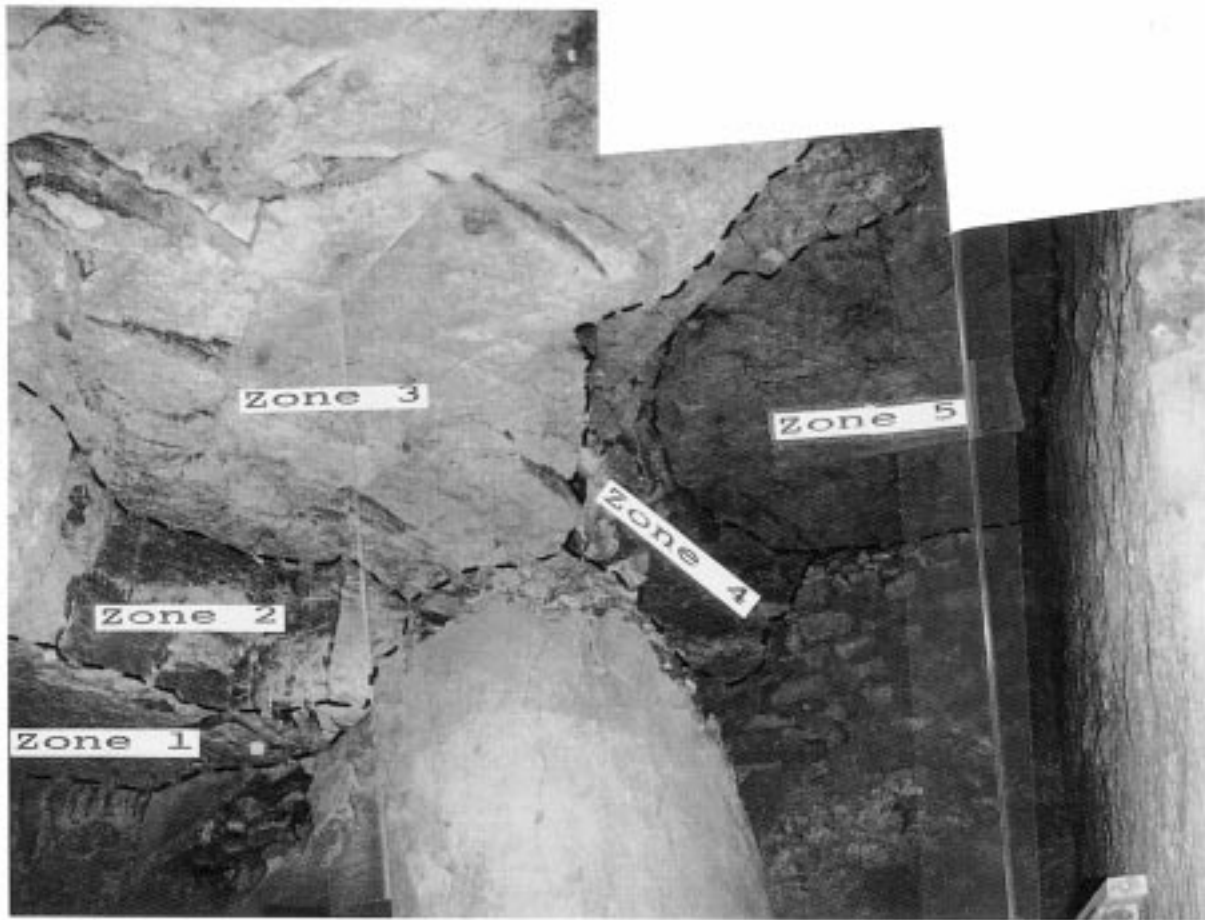


Fig. 8. A photograph showing the transition from the original roof (zone 1) to the uppermost level of the loosened zone (zone 5). The support pillar is in the right side of the picture.

limits of the interbedded marl indicate relatively low plasticity and low swelling potential.

The discontinuities were mapped on the failed roof surface as well as on exposed river bed outside the underground excavation. Scan lines were placed both underground (on the roof) and on the outcrop outside and results were compared. Three principal joint sets are defined (Table 1). The joints are very persistent with trace line length greater than the opening dimension and are treated therefore as continuous infinite planes. The joints are clean and tight with planar surfaces. The roughness of the joint planes was estimated using a profilometer. Ten measured profiles were compared with JRC standards [10] and the mean JRC value is estimated at 8–10. The residual friction angle of the joints was estimated using tilt tests performed on mating saw cut joint planes. The mean residual friction angle is between 35 and 36°. Tilt tests performed on mating natural joints as found in the field yielded values between 49–71°. In order to assess the peak fric-

tion angle which was available at the time of deformation the empirical criterion of Barton [11] is used: $\tau = \sigma_n \tan[\text{JRC} \log_{10}(\text{JCS}/\sigma_n) + \phi_r]$ with the following input parameters: $\text{JRC} = 8\text{--}10$; $\text{JCS} = 7 \text{ MPa}$; $\sigma_n = 0.5\text{--}2.5 \text{ MPa}$; $\phi_r = 35^\circ$. The maximum normal stress active on the joints (σ_n) is a function of beam thickness and is estimated here from output of Voussoir beam analysis [4] for a beam with span of 7 m and thickness between 0.5 and 2.5 m. Using the criterion of Barton the dilation angle is expected to vary between 3.6 and 11.4° and, therefore, the peak friction angle is expected to vary between 38.6 and 46.4°. Estimation of input data for rock mass classification methods [10, 12, 13] yields an estimated Q value between 0.4 and 4.0 and an estimated RMR value of 43. These values indicate a fair to poor rock with an expected stand up time of 1 to several days. The estimated rock mass classification values help explain the historic failure; with the given lithological conditions and considering modern experience we do not expect the rock mass to have been able to sustain the loads which were induced by the attempted excavation for a significant period of time.

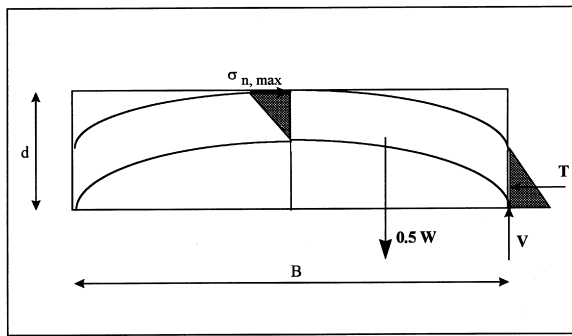
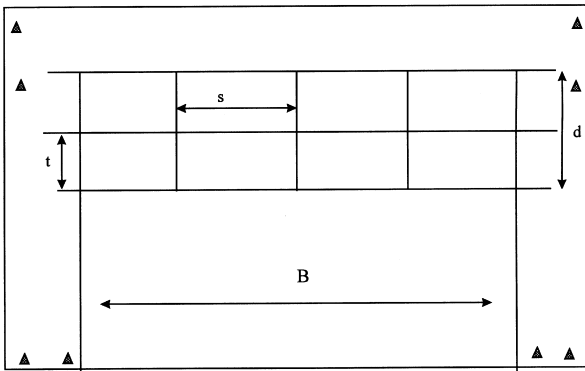
Table 1. Principal joint sets in the underground opening

	Dip	Strike direction	Room	Mean spacing (cm)
J1	90	039–061	1, 2, 3, 4	20
J2	90	124–127	1, 2	25
J3	90	107–112	3, 4	60

CLASSIC VOUSSOIR BEAM ANALYSIS

The general geometry of a laminated Voussoir beam is shown in Fig. 9(a). The principal geometric par-

a Laminated Voussoir beam geometry and geometrical parameters for DDA



b Voussoir beam geometry and load specification for roof beam analysis

Fig. 9. (a) Laminated Voussoir beam geometry. The small triangles are fixed point location as used in DDA and (b) Voussoir beam geometry and load specifications for roof beam analysis [5].

ameters are beam span (B), overall beam height (d), individual layer thickness (t) and joint spacing (s). This general model is used in DDA with fixed point location as marked in Fig. 9(a) by the small triangles. The geometry of a “classic” Voussoir beam is shown in Fig. 9(b) [5], where the beam consists of a single layer and the number of intermediate joints is irrelevant. Therefore the only geometric parameters in the classic analysis are beam span (B) and beam height (d).

The assumption in the classic model is that at equilibrium the lateral thrust is not transmitted either uniformly or axially through the beam cross section [5]. The section of the beam transmitting lateral load is assumed to be parabolic as shown in Fig. 9(b). Another assumption is that the central transverse crack determines the deformational behavior of the beam across which the stress distribution is triangular [5] and therefore the problem is analyzed according to the assumed load distribution and line of action of the resultant force as shown in Fig. 9(b). The assumptions concerning the parabolic shape of the compressive zone and the triangular load distribution on the abutments and on the central section are intuitively appealing considering the mechanism of slight deflection of the central section, which is followed by maximum compression at the hinge zones, namely

uppermost level at central section and lowermost level at both abutments. A good summary of the iterative procedure is provided by Brady and Brown [5].

The maximum axial stress (σ_n) in the classic Voussoir beam analysis [4] was computed for beam spans ranging between 3 and 9 m and beam thickness between 0.25 and 2.5 m (Fig. 10). It can be seen that in general σ_n increases with increasing beam span and decreases with increasing beam thickness. The calculated results, however, are only valid for a beam consisting of a single layer. The case of Tel Beer Sheva is shown in the heavy line in Fig. 10 for a beam span of 7 m. The value of σ_n , obtained for an individual layer thickness of 0.25 m, is 2.45 MPa. For a single layer beam with thickness of 2.5 m, σ_n is 0.244 MPa. At Tel Beer Sheva the average bed thickness is 0.5 m. Assuming that each bed transmits axial thrust independently from the neighboring layers above and below, σ_n within a single layer should be 1.22 MPa. These values are significantly lower than the unconfined compressive strength of the rock which is about 7 MPa and, therefore, the beam should be considered safe against failure by local crushing at hinge zones, according to this analysis.

Another possible failure mechanism is by shear along the abutments. Assuming that the joint and abutment planes have zero cohesion, the factor of safety against failure in shear along the abutments is given by [5]:

$$F.S. = \frac{T \tan \phi}{V} = \frac{0.5\sigma_n n d \tan \phi}{0.5\gamma B d} = \frac{\sigma_n}{\gamma B} n \tan \phi$$

where T = resultant horizontal (normal) force; V = resultant vertical (shear) force; ϕ = available friction angle along abutment wall or vertical joint; σ_n = maximum axial stress; n = assumed load/depth ratio (compressive zone thickness is given by $n \times d$); d = beam thickness; B = beam span and γ = unit weight of rock. The sensitivity of the factor of safety to beam thickness (d) is not apparent from inspection of the expression above, since the dependence is through the magnitude of σ_n which is a function of d (Fig. 10). In Fig. 11 the factor of safety against shear along the abutments is calculated for different values of ϕ and beam thickness. Indeed the sensitivity of the factor of safety to beam thickness is quite high and a logarithmic scale is used for better resolution. Clearly the factor of safety against shear decreases with increasing beam thickness, since the magnitude of the axial thrust decreases with increasing beam thickness (Fig. 10).

The available friction angle for Tel Beer Sheva was estimated between 38.6 and 46.4° using the empirical criterion of Barton [11]. A heavy line representing available friction angle (ϕ_{avail}) of 40° is shown in Fig. 11, a fair assumption regarding ϕ_{avail} in the field. With a given friction angle of 40° the opening should be safe against shear along the vertical abutments, for beam thickness between 0.25 and 2.5 m. In fact, the

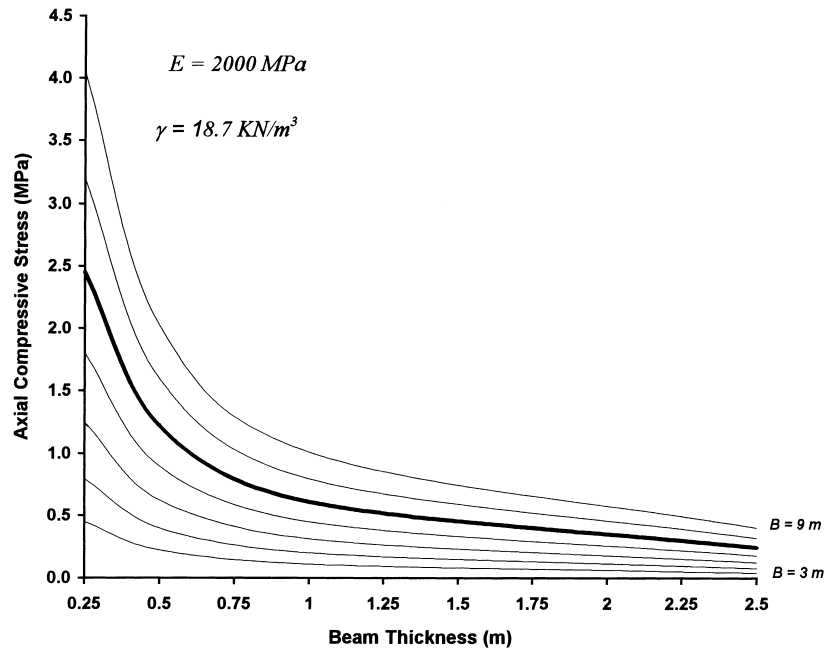


Fig. 10. The relationship between maximum horizontal compressive stress in beam and beam thickness for various roof span values (B), determined using Voussoir beam analysis [4]. The case of Tel Beer-Sheva ($B = 7 \text{ m}$) is shown using bold line.

required friction angle for stability according to Voussoir beam analysis is not greater than 36° , for every beam thickness.

The results obtained using classic Voussoir beam analysis cannot explain the failure. The local compression which develops at the hinge zones is too low compared to the available compressive strength; the shear stress which develops along the vertical abut-

ments due to beam weight is lower than the shear strength of the abutments, considering a conservative estimate of friction angle. We must conclude, therefore, that the approach taken by classic Voussoir beam analysis [4], which ignores the influence of joint spacing and the existence of multiple beds is unconservative and should not be applied in practice for the analysis of a laminated Voussoir beam.

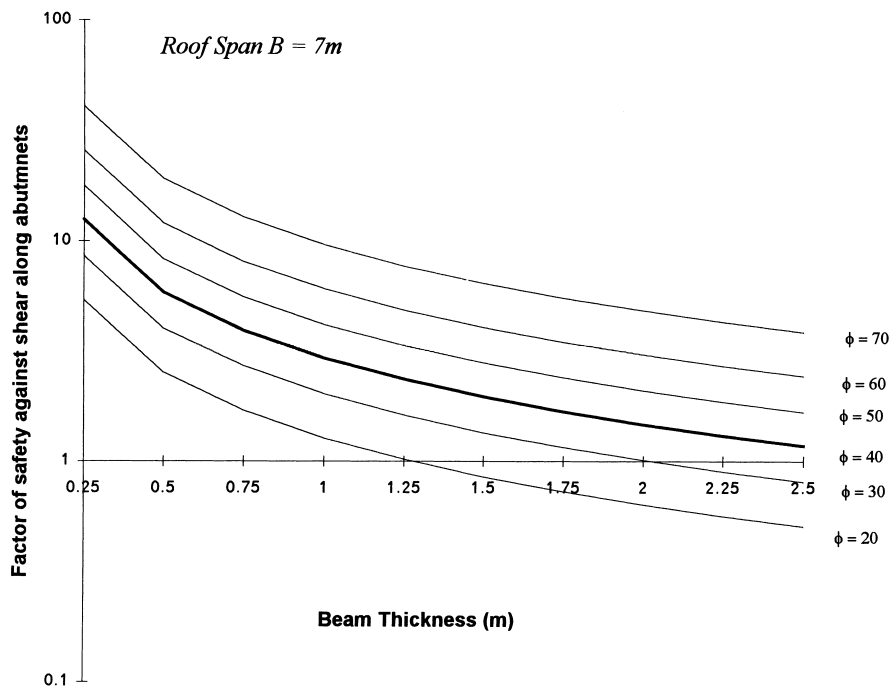


Fig. 11. Factor of safety against shear along abutments for different values of beam thickness and a constant roof span of 7 m, using Voussoir beam analysis [4]. The results indicate that the roof is safe with respect to shear along the abutments provided that the available friction angle is greater than 40° (bold line).

DISCONTINUOUS DEFORMATION ANALYSIS

Theory and practice of DDA: A brief background

In order to investigate the influence of multiple beds and joints on the stability of a Voussoir beam, discontinuous deformation analysis is used. DDA was developed by Shi [8,9] and its validity was tested for cases where analytical solutions were available by Yeung [14]. The theory and mathematical formulation of DDA for backward and forward modeling of discontinuous media are summarized by Shi and Goodman [15,16] and Shi [17]. The applicability of DDA for the case of a simple three-hinged beam was investigated by comparing the numerical output of rotation vs time with analytical results, using two assumptions concerning the reaction forces [18]. The numerical results of DDA were found to agree extremely well with analytical predictions, provided that small time steps were used, due to DDA's first order approximations. Application of DDA for the case of horizontally bedded and vertically jointed roof was demonstrated by Yeung and Goodman [19]. Yeung [20] studied numerically the effect of friction angle on various rock bolting schemes in such a rock mass. A block fracturing algorithm was recently implemented in DDA [21,22] using a three parameter Mohr–Coulomb criterion (cohesion, friction and tensile strength) where fracturing can be either in shear or in tension. Furthermore, a sub-blocking capability was developed [21,22] which allows better analysis of stress and strain distributions within otherwise simply deformable DDA blocks. Validation of DDA using *real* case studies, however, has rarely been attempted. Chang and Monteiro [23], for example, have investigated the failure of St. Francis Dam using a finite element mesh superimposed on DDA blocks and found that the correct failure modes were generally detected by DDA, but concluded that complete three-dimensional analysis would have been more suitable for the problem at hand.

DDA in its current implementation is two-dimensional and is therefore applicable for certain two-dimensional sections of otherwise a three-dimensional problem. In this research a C version of the original DDA code [8,9] is used with computer interface modifications performed by MacLaughlin and Sitar at Berkeley [24] who also provide a concise review of the method.

The DDA method incorporates dynamics, kinematics and elastic deformability of the rock and models actual displacements of individual blocks in the rock mass. The formulation is based on minimization of potential energy and uses a “penalty” method to prevent penetration of blocks. Numerical penalties in the form of stiff springs are applied at the contacts to prevent interpenetration or tension between blocks. Tension or penetration at the contacts will result in expansion or contraction of these springs, a process which requires energy; the mini-

um energy solution is therefore one with no tension or penetration. When the system converges to an equilibrium state, however, there are inevitable penetration energies at each contact, which balance the contact forces. The energy of the penetration (the deformation of the springs) can be used to calculate the normal and shear contact forces [14]. Shear displacement along boundaries is modeled in DDA using the Coulomb–Mohr failure criterion. The fixed boundaries are implemented using the same penalty method formulation: stiff springs are applied at the fixed points. Since displacement of the fixed points requires great energy, the minimum energy solution will not permit fixed point displacement.

The blocks are simply deformable: stresses and strains within a block are constant across the whole region of the block. This feature requires a minimum number of blocks in the mesh in order to accurately calculate stress and strain distribution throughout the medium. This disadvantage can be overcome by implementing sub-block capabilities [21,22] where blocks are discretized into sub-blocks. The problem of simply deformable blocks is apparently solved in the new manifold method [25] in which a mathematical mesh “covers” the DDA mesh. However in the current development stage friction is not implemented, and therefore the scope of back analysis using the manifold method is naturally more limited at present.

DDA experiments

The carefully documented geometry of the failed roof is used here in back analysis of the failure. The active span is assumed to be of 7 m as before, but a distinction is made now between overall beam thickness and individual layer thickness. The overall beam thickness is considered here to be represented by the height of the loosened zone, about 2.5 m (Fig. 5), and the individual layer thickness is taken as the average bed thickness, about 50 cm. The geometric parameter which is used as a variable is the mean joint spacing and the mechanical parameter which is used as a variable is joint friction.

DDA runs are performed for the general geometry which is schematically shown in Fig. 9(a), where fixed point location is marked by small triangles. In each analysis a constant mean joint spacing value (s) is used and the value of friction angle along the boundaries is changed until the system shows stability. The stability of the roof is defined by a specified value of maximum deflection at the mid-section of the beam, the magnitude of which would not change regardless of the number of time steps. In this research the roof is considered to arrive at stability when a maximum deflection of up to 5.5 cm is detected at the mid-section, after at least 25 time steps.

The size of the time step and the penalty value are automatically optimized and updated between time steps by the current implementation of DDA (DDA

Table 2. Results of DDA experiments for a laminated Voussoir beam with span of 7 m, overall thickness of 2.5 m and layer thickness of 0.5 m. The input material properties are: mass per unit area = 1900 kg/m²; weight per unit area = 18.7 kN/m²; elastic modulus = 2 × 10⁶ kN/m; Poisson's ratio = 0.1

	Mean joint spacing (cm)						
	25	50	87.5	116	175	350	700
No. blocks in layer	28	14	8	6	4	2	1
No. blocks in beam	140	70	40	30	20	10	5
Block dimension (s/t)	0.5	1.0	1.75	2.33	3.5	7	14
$\phi_{\text{required}}^{\circ}$	80	55	40	30	25	45	90

version 1996). At the beginning of a time step, the locked directions of closing contacts are selected. A contact spring is applied in each locked direction to prevent penetration along the spring directions. The submatrices of contact springs are added to the simultaneous equilibrium equations prior to solving the equations. After the equations are solved to obtain the new block system configuration, if there is penetration at a contact where no contact spring is used, the forward modeling program (DF) goes back to the beginning of the time step and applies a contact spring; if there is a contact spring having tension higher than the allowable tension calculated from the tensile strength, DF goes back to the beginning of the time step and deletes this contact spring. This procedure of repeated lock selections is called "open-close" iterations. The general equilibrium equations are formulated and solved iteratively until there are no penetrations and no spring tension higher than the allowable at all contacts. At the end of the time step, all the blocks are in equilibrium with appropriate contact conditions. Because the penalty value is optimized and updated by DDA (Version 1996) automatically between time steps, we did not experiment with the sensitivity of the analysis predictions to the penalty value. As a general rule however, a suitable value for the stiffness of contact spring (F/L) is $(E_0)(L_0)$ where E_0 is the Young's modulus of the blocks and L_0 is the average block "diameter".

The maximum allowable displacement ratio, namely the maximum allowable displacement per time step divided by half the vertical dimension of the region, is set to 0.01. In the analyzed case study the maximum allowable displacement per time step is 3.5 cm.

The joints are considered planar and cohesionless with zero tensile strength, an honest representation of the situation in the field. The friction angle of vertical joints and horizontal bedding planes is assumed equal, merely for simplicity; this is by no means a limitation of the method. The input material parameters are: mass per unit area = 1900 kg/m²; weight per unit area = 18.7 kN/m²; Young's modulus, $E = 2 \cdot 10^6$ kN/m and Poisson's ratio, $\nu = 0.1$. Seven mean joint spacing values are analyzed: $s = 25, 50, 87.5, 116, 175, 350$ and 700 cm (Table 2). The roof is modeled for friction angle values between 20 and 90°. The maximum deflection at mid-section for a given friction angle value is noted in each run (Table 3). Typically

stability and cease of motion is detected after 12–16 time steps. The results of the seven DDA experiments are listed in Tables 2 and 3.

DDA results

Three graphical outputs of DDA experiments are shown in Fig. 12. In Fig. 12(a) the joint spacing is 25 cm, similar to the mean joint spacing of joint sets 1 and 2, with a block dimension ratio lower than 1 ($s/t = 0.5$). The response of the roof to an available friction angle of 40° is shown in Fig. 12(a.1). The roof shears as one beam along the abutments, although the individual blocks are free to displace across any joint. This result is in agreement with the empirical and numerical results of Ran *et al.* [7] who found that the resistance to shear sliding across the abutments is lower than across the mid-section; a beam containing multiple midjoints of similar properties is therefore expected to shear along the abutments and not along the midjoints. When the available friction angle is 50° onset of arching is indicated by less vertical displacement along the abutments, and greater deflection at mid section (Fig. 12(a.2)). In order to satisfy our stability criterion of maximum deflection at mid section ($u_{\text{max}} \leq 5.5$ cm) a friction angle of 80° is required (Fig. 12(a.3)), although available friction angles of 60 and 70° yield stable arching with maximum deflec-

Table 3. Concentrated output of DDA experiments: maximum deflection at mid-section (cm) after up to 25 time steps. Maximum displacement per time step = 3.5 cm

	Spacing (cm)						
	25	50	87.5	116	175	350	700
$\phi_{\text{avail.}} = 20^{\circ}$	66	72	90	16	89		
$\phi_{\text{avail.}} = 25^{\circ}$				10	0		
$\phi_{\text{avail.}} = 30^{\circ}$	60	60	83	5.5		60	
$\phi_{\text{avail.}} = 35^{\circ}$			12				
$\phi_{\text{avail.}} = 40^{\circ}$	50	36	5.5			10	
$\phi_{\text{avail.}} = 45^{\circ}$						0	
$\phi_{\text{avail.}} = 50^{\circ}$	39	14					
$\phi_{\text{avail.}} = 55^{\circ}$		5.5					
$\phi_{\text{avail.}} = 60^{\circ}$	12						
$\phi_{\text{avail.}} = 65^{\circ}$							
$\phi_{\text{avail.}} = 70^{\circ}$	12						
$\phi_{\text{avail.}} = 75^{\circ}$	12						
$\phi_{\text{avail.}} = 80^{\circ}$	5.5						100
$\phi_{\text{avail.}} = 85^{\circ}$							100
$\phi_{\text{avail.}} = 90^{\circ}$							0

tions of 12 cm (Table 3). The response of the roof to a mean spacing value of 50 cm, somewhat lower than the mean spacing value of joint set 3, is shown in Fig. 12(b), where the block dimension ratio (s/t) equals 1.0 (the blocks are equi-dimensional).

Transition from simple shear along the abutments to arching is detected with available friction angle of 30° (Fig. 12(b.1)) by greater deflection of the mid-section with respect to the abutments. When the available friction angle is 50° the roof is safe (Fig. 12(b.2)) but

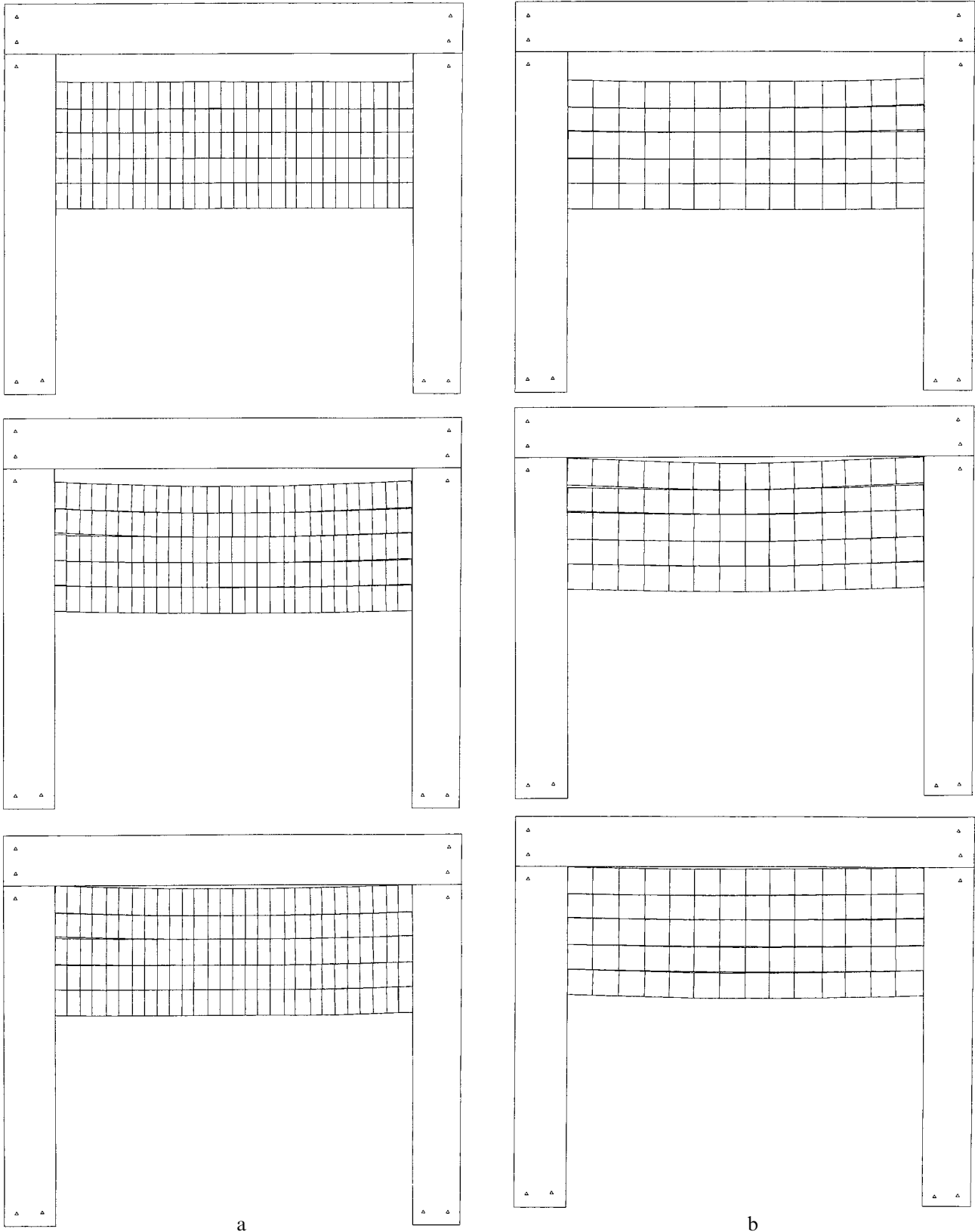


Fig. 12(a, b).

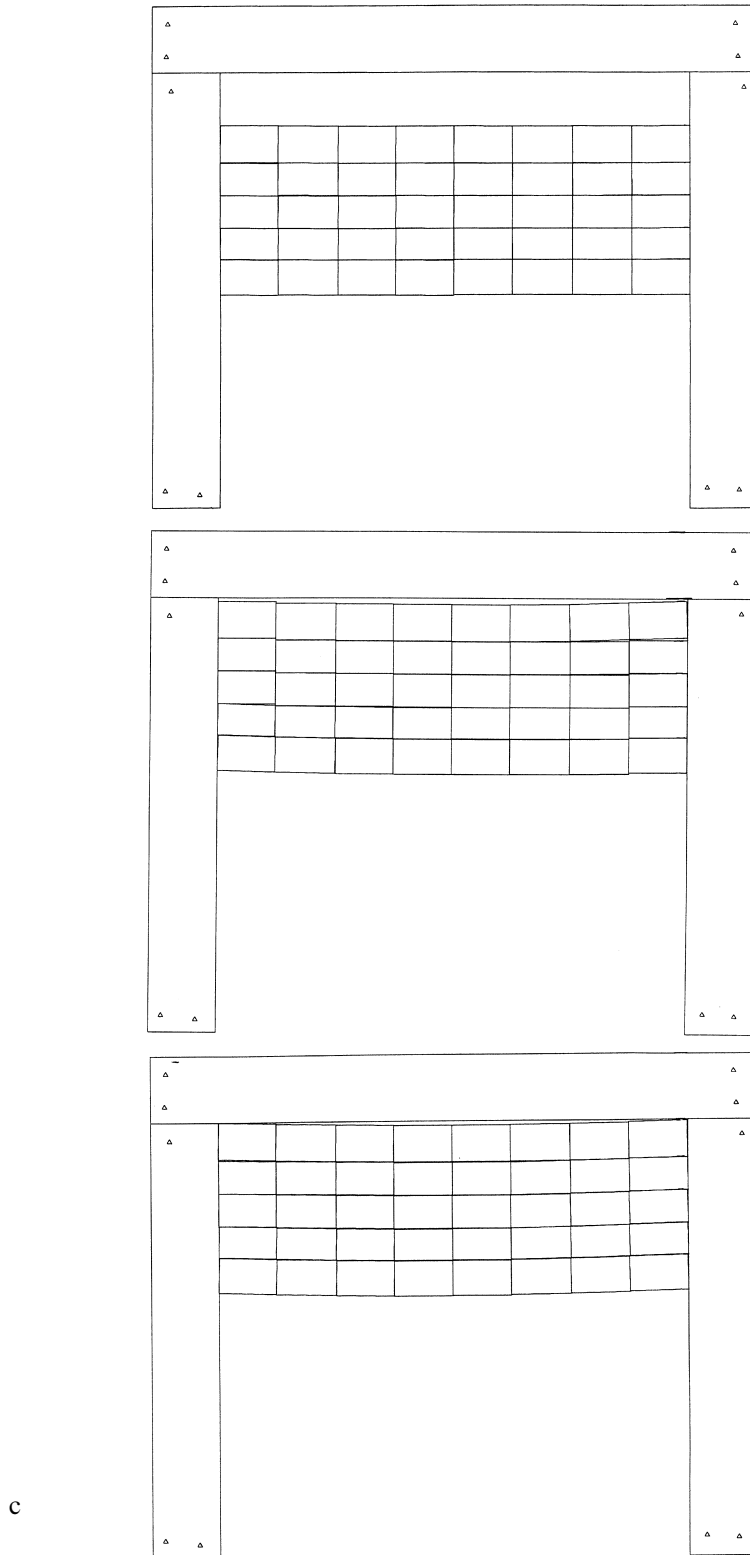


Fig. 12. Results of DDA experiments for roof span of 7 m, loosened zone thickness of 2.5 m and individual beam thickness of 0.5 m. (a) $s = 25$ cm: $\phi_{\text{available}} = 40^\circ$, shear along abutments; $\phi_{\text{available}} = 50^\circ$, onset of arching deformation; $\phi_{\text{available}} = 80^\circ$, stable arching with maximum vertical deflection at mid-section ($u_{\text{max.}}$) of 5.5 cm, (b) $s = 50$ cm: $\phi_{\text{available}} = 30^\circ$, shear along abutments coupled with arching; $\phi_{\text{available}} = 50^\circ$, arching ($u_{\text{max.}} = 12$ cm); $\phi_{\text{available}} = 55^\circ$, stable arching ($u_{\text{max.}} = 5.5$ cm), (c) $s = 88$ cm: $\phi_{\text{available}} = 30^\circ$, shear along abutments; $\phi_{\text{available}} = 35^\circ$, arching ($u_{\text{max.}} = 12$ cm); $\phi_{\text{available}} = 40^\circ$, stable arching ($u_{\text{max.}} = 5.5$ cm).

the deflection exceeds the specified limit ($u_{\text{max}} = 12$ cm), which is completely satisfied with available friction angle of 55° (Fig. 12(b.3)). In Fig. 12(c) a mean spacing value of 87.5 cm is tested,

somewhat higher than the mean spacing of joint set 3. In this geometry the block dimension ratio is greater than 1 ($s/t = 1.76$) and this has a great effect on overall stability: while with $\phi_{\text{avail.}} = 30^\circ$ the roof

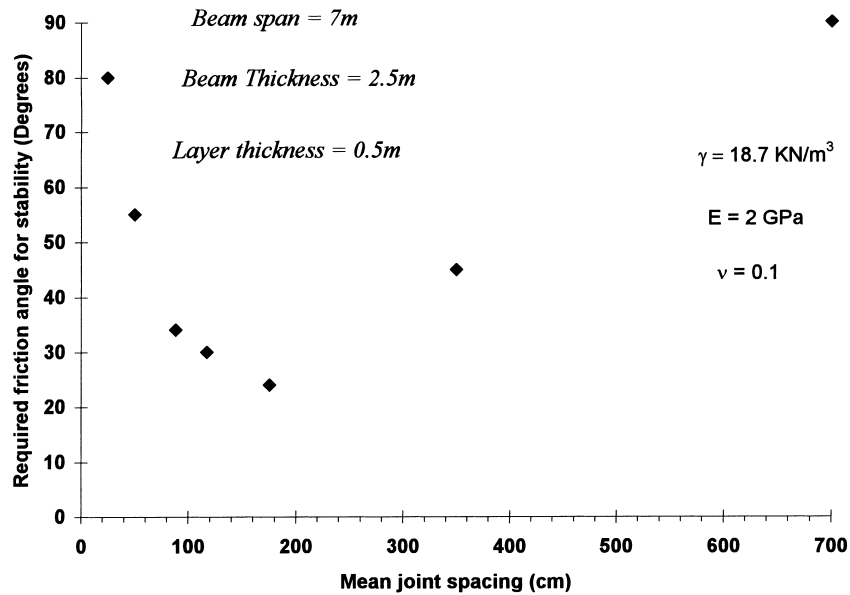


Fig. 13. Required friction angle for stable arching ($u_{\max} \leq 5.5$ cm) as a function of joint spacing in a layered Voussoir beam with a constant layer thickness of 50 cm.

slides along the abutments as a single beam (Fig. 12(c.1)), with $\phi_{\text{avail.}}$ of 35° stable arching is detected (Fig. 12(c.2)) and the stability criterion is fully satisfied with $\phi_{\text{avail.}} = 40^\circ$ (Fig. 12(c.3)). When the block dimension ratio further increases to $s/t = 3.5$ ($s = 175$ cm) the arching mechanism is extremely efficient and transition from shear along the abutments to complete stability is achieved when $\phi_{\text{avail.}}$ increases from 20° ($u_{\max} = 89$ cm) to 25° ($u_{\max} = 0$), see Table 3.

The analyses shown in Fig. 12 suggest that with increasing block ratio (s/t) the resistance to shear along the abutments is improved, where everything else is kept equal. For beams of constant thickness this result implies that shear along the abutments is less likely with increasing joint spacing. This result is in disagreement with the empirical and numerical data of Ran *et al.* [7] who found that with increasing length of midblocks the possibility for shear along the abutments increases. However it should be noted that the physical experiments and non-linear FEM models of Ran *et al.* [7] were limited to a single layered Voussoir beam, as in the case of classic Voussoir beam analysis [4].

DISCUSSION

The failure of a horizontally bedded and vertically jointed roof of an ancient water storage reservoir is back analyzed here using the classic Voussoir beam analysis [4] and the DDA method [8, 9]. The unconfined compressive strength of the rock is higher than the estimated axial thrust in the beam and we, therefore, explore the possibility of failure by shear along the abutments, rather than by crushing at the hinge zones. Furthermore, application of the original DDA

code [8, 9, 24] with no block fracturing capabilities is sufficient for the analysis of this case, as no internal block crushing is expected.

The classical Voussoir beam analysis [4], although insightful, is not valid for the present case because it considers a beam consisting of a single layer, and ignores joint spacing. Indeed, the required friction angle against shear sliding along the abutments according to that analysis is 36° (Fig. 11), while the available friction angle is estimated between 38.6 and 46.4° . This result also implies that the classic Voussoir beam analysis is in fact unconservative in the case of a laminated beam, a very common situation in mining through sedimentary strata.

The limitations of classical Voussoir beam analysis are overcome here by means of the DDA method [8, 9], in which the influence of both joint spacing and load transfer from overlying layers in a laminated beam can be modeled with confidence regarding computation accuracy.

The results of seven DDA experiments are shown graphically in Fig. 13 where the required friction angle is plotted against mean joint spacing. Consider Tel Beer Sheva, where the mean joint spacing in rooms 1 and 2 is 25 cm (Fig. 3). In this configuration onset of arching was detected with $\phi_{\text{avail.}} = 40^\circ$ but the roof was not stable (Fig. 12(a.1)). The roof stabilized with available friction angle greater than 60° but the deflection at mid-section was excessive, in the order of 12 cm (Table 3). The deflection at mid-section was acceptable with available friction angle of 80° , yet the roof would not have collapsed according to DDA analysis had the available friction angle been greater than 60° . The stability of the roof is much improved with a mean spacing of 50 cm, where a friction angle of 55° is required. With a mean joint spacing of 88 cm the roof

is completely stable with required friction angle of 34° only.

The results of these three DDA experiments are sufficient for back analysis of the failure. Considering Fig. 3, joint sets 1 and 2 are predominantly represented in the roof of the opening with occurrences of joint set 3 in room 3. The most probable mean joint spacing value in most two-dimensional sections of the failed roof is therefore in the order of 25 cm (see, for example Fig. 4). With this joint spacing the required friction angle according to DDA is greater than 60° , but the estimated friction angle which is available is between 38.6 and 46.4° , as noted earlier. It was shown in a series of DDA experiments (Fig. 12) that shear deformation along the abutments preceded arching deformation and development of high compressive stresses at hinge zone, when the available friction angle was lower than the required value. Therefore, it would be safe to assume that failure in shear must have ensued as soon as construction of the active spans was attempted by the ancient engineers. The roof has collapsed into a three-dimensional dome arriving at a new equilibrium after the failure. In order to improve stability, the ancient engineers erected the massive support pillar below the center of the dome, with vertical side extensions required for support of unstable step zones (zone 4) in the roof (Figs 6 and 7).

The results of this study can be used to further understand the influence of joint spacing, or block shape, on overall stability of a laminated Voussoir beam. The results of DDA (Fig. 13) clearly indicate that the required friction angle for stability decreases with increasing block length, or joint spacing. However, the empirical function is not monotonously decreasing but presents a minimum, when the number of blocks in an individual layer is 4 (Table 2). When the number of blocks further decreases, and block length or joint spacing increases, the stability of the roof decreases and the required friction angle for stability increases. Ultimately, when each individual layer consists of a single block the required friction angle is 90° because the abutment walls are vertical with zero cohesion. It should be recalled, however, that with decreasing number of blocks the accuracy of stress distribution in the mesh decreases since the blocks are simply deformable in DDA, as explained before. In order to check the exact location of the minimum point in the empirical function (Fig. 13) it would be required to use a finite "cover" coupled with DDA mesh, using, for example the new manifold method [25].

The result of this study can be qualitatively rationalized as follows: with increasing joint spacing the moment arm length in individual blocks increases and the arching mechanism by which axial thrust is transmitted through the blocks to the abutments is enhanced. However, above a limiting value of block length, found here to be represented by a layer consisting of four blocks, the weight of the overlying blocks

becomes more dominant, and the stabilizing effect of greater axial thrust is weakened by the destabilizing effect of dead load transfer from the weight of overlying blocks. Finally, when a single layer consists of a single block which is not clamped at the ends arching deformation is unlikely, due to the relatively high stiffness of individual layers.

SUMMARY AND CONCLUSIONS

A roof failure of an ancient water reservoir, excavated through horizontally bedded and vertically jointed chalk, was analyzed using Voussoir beam analysis [4] and the DDA method [8, 9]. The analytical study was focused on shear failure along the vertical abutments due to developed vertical shear stresses, rather than on failure by crushing at the hinge zones due to induced axial compressive stresses. DDA experiments have shown that when the available shear strength of the abutments is too low the composite roof shears as a single beam along the vertical abutments, in agreement with physical experiments and non-linear finite element analyses [6, 7] which showed that maximum vertical shear stress develops at the edge of the Voussoir beam. When the shear strength of the abutment wall is sufficiently high arching deformation ensues, indicated in DDA experiments by greater deflection of the roof at mid-section and minimal vertical displacement across the abutments.

The application of classic Voussoir beam analysis [4] to the case of a laminated Voussoir beam proved inappropriate and unconservative. The required friction angle against shear along the abutments is 36° using the iterative procedure, while the available friction angle in the field is estimated between 38.6 and 46.4° . The discrepancy is explained by the insensitivity of the iterative procedure to joint spacing and joint friction, as well as its limited applicability for the case of a single layer Voussoir beam.

Using the DDA method, the required friction angle against shear along the abutments as a function of joint spacing is explored. For the available mean joint spacing in the field (25 cm) the required friction angle by DDA is greater than 60° , a shear strength which was not available at the time of construction, and hence the failure.

The influence of joint spacing and block shape on stability is also explored using DDA. It is found that with increasing joint spacing or block length (when individual layer thickness is kept constant) the resistance to shear along the abutments improves up to a critical value of joint spacing or block length, beyond which the composite beam becomes less stable. This is rationalized by the coupled effect of two competing forces which act in the composite beam: one is the stabilizing axial thrust which is enhanced with increasing moment arm or block length, the other is the destabilizing effect of the weight of overlying blocks which increases with increasing block length or joint spacing.

Acknowledgements—This research was funded by Israel National Parks Authority through contract # 390 and their support is hereby acknowledged. We thank Prof. D. Bahat for helpful discussions; Prof. J. A. Hudson and another anonymous reviewer are thanked for their comments.

Accepted for publication 11 July 1997

REFERENCES

- Obert, L. and Duvall, W. I., *Rock Mechanics and the Design of Structures in Rock*. Wiley, New York, 1967, p. 650.
- Goodman, R. E., *Introduction to Rock Mechanics*, 2nd edn. Wiley, New York, 1989, p. 562.
- Evans, W. H., The strength of undermined strata. *Trans. Inst. Min. Metall.*, 1941, **50**, 475–532.
- Beer, G. and Meek, J. L., Design curves for roofs and hanging walls in bedded rock based on Voussoir beam and plate solutions. *Trans. Inst. Min. Metall.*, 1982, **91**, A18–22.
- Brady, B. H. G. and Brown, E. T., *Rock Mechanics for Underground Mining*, 2nd edn. Chapman and Hall, London, 1993, p. 571.
- Passaris, E. K. S., Ran, J. Q. and Mottahed, P., Stability of the jointed roof in stratified rock. *Int. J. Rock Mech. Min. Sci. Geomech. Abstr.*, 1993, **30**(7), 857–860.
- Ran, J. Q., Passaris, E. K. S. and Mottahed, P., Shear sliding failure of the jointed roof in laminated rock mass. *Rock Mech. Rock Eng.*, 1991, **27**(4), 235–251.
- Shi, G. -H., Discontinuous deformation analysis: A new numerical model for the statics and dynamics of block systems. Ph.D. thesis, University of California, Berkeley, 1988.
- Shi, G. -H. *Block System Modeling by Discontinuous Deformation Analysis*. Computational Mechanics Publications, Southampton, 1993, p. 209.
- Barton, N. R., Lien, R. and Lunde, J., Engineering classification of rock masses for the design of tunnel support. *Rock Mech.*, 1974, **6**(4), 189–239.
- Barton, N. R., Review of a new shear strength criterion for rock joints. *Eng. Geol.*, 1973, **8**(4), 287–332.
- Bieniawski, Z. T., Engineering classification of jointed rock masses. *Trans. S. Afr. Inst. Min. Metall.*, 1976, **74**(4), 335–344.
- Barton, N. R., *Predicting the Behavior of Underground Openings in Rock*, vol. 172. NGI Publ., 1987, p. 61.
- Yeung, M. R., Application of Shi's discontinuous deformation analysis to the study of rock behavior. Ph.D. thesis, University of California, Berkeley, 1991.
- Shi, G.-H. and Goodman, R. E., Two-dimensional discontinuous deformation analysis. *Int. J. Numer. Anal. Methods Geomech.*, 1985, **9**(4), 541–556.
- Shi, G.-H. and Goodman, R. E., Generalization of two-dimensional discontinuous deformation analysis for forward modeling. *Int. J. Numer. Anal. Methods Geomech.*, 1989, **13**(4), 359–380.
- Shi, G.-H., Discontinuous deformation analysis: A new numerical model for the statics and dynamics of deformable block structures. *Eng. Comput.*, 1992, **9**(4), 157–168.
- Yeung, M. R., Analysis of a three-hinged beam using DDA. In *Proceedings of the First International Forum on DDA and Simulations of Discontinuous Media*, ed. M. R. Salami and D. Banks. TSI Press, Albuquerque, 1996, pp. 462–469.
- Yeung, M. R. and Goodman, R. E., Multi-block stability analysis using the DDA method. In *Fractured and Jointed Rock Masses*, ed. L. R. Myer, N. G. W. Cook, R. E. Goodman and C.-F. Tsang, Balkema, Rotterdam, 1995, pp. 701–707.
- Yeung, M. R., Analysis of a mine roof using the DDA method. *Int. J. Rock Mech. Min. Sci. Geomech. Abstr.*, 1993, **30**(7), 1411–1417.
- Lin, C. T., Amadei, B., Jung, J. and Dwyer, J., Extension of discontinuous deformation analysis for jointed rock masses. *Int. J. Rock Mech. Min. Sci. Geomech. Abstr.*, 1996, **33**(7), 671–694.
- Amadei, B., Lin, C. and Dwyer, J., Recent extensions to the DDA method. In *Proceedings of the First International Forum on DDA and Simulations of Discontinuous Media*, ed. M. R. Salami and D. Banks. TSI Press, Albuquerque, 1996, pp. 1–30.
- Chang, C.-T. and Monteiro, P. J. M., Reassessment of the St. Francis dam failure using finite element meshed discontinuous deformation analysis. In *Proceedings of the First International Forum on DDA and Simulations of Discontinuous Media*, ed. M. R. Salami and D. Banks. TSI Press, Albuquerque, 1996, pp. 295–301.
- MacLaughlin, M. M. and Sitar, N., Discontinuous deformation analysis for the windows PC environment, UC-Berkeley Version 1.1. Geotechnical Engineering Report No. UCB/GT/95-04, Berkeley, 1995, p. 23.
- Shi, G.-H., Manifold method. In *Proceedings of the First International Forum on DDA and Simulations of Discontinuous Media*, ed. M. R. Salami and D. Banks. TSI Press, Albuquerque, 1996, pp. 52–262.